Available online at www.sciencedirect.com

SCIENCE DIRECT®

Earth and Planetary Science Letters 229 (2004) 31–43

EPSL

www.elsevier.com/locate/epsl

A new three-axis vibrating sample magnetometer for continuous high-temperature magnetization measurements: applications to paleo- and archeo-intensity determinations

Maxime Le Goff*, Yves Gallet

Département de Géomagnétisme et Paléomagnétisme, UMR CNRS 7577, Institut de Physique du Globe de Paris, 4 Place Jussieu, 75252 Paris cedex 05, France

Received 13 May 2004; received in revised form 18 October 2004; accepted 18 October 2004
Available online 21 November 2004
Editor: R.D. van der Hilst

Abstract

We have developed a new three-axis vibrating sample magnetometer, which allows continuous high-temperature magnetization measurements of individual cylindrical ~0.75 cm^3 samples up to ~650 °C and the acquisition of thermoremanent magnetization (TRM) in any direction and field intensity up to 200 μT. We propose a fast (less than 2.5 h) automated experimental procedure adapted from Boyd's [Nature 319 (1986) 208–209] modified version of the Thellier and Thellier [Ann. Geophys. 15 (1959) 285–376] method which provides continuous intensity determinations over a large (typically 300 °C) temperature interval for each sample. This procedure allows one to take into account both the cooling rate dependence of TRM acquisition and anisotropy of TRM. Several examples of analyses of ancient magnetization demonstrate the quality and reliability of the data and illustrate the promising potential of this new instrument in paleo- and archeomagnetism.

Keywords: magnetometer; paleo-intensity; archeomagnetism; cooling rate; anisotropy

1. Introduction

Deciphering the dynamical processes generating the Earth's magnetic field requires a complete description both in direction and intensity of the temporal geomagnetic variations at various time scales. Our knowledge of geodynamo evolution is presently strongly biased in favour of the directional variations as paleo- and archeo-intensity data are still scarce and not always of sufficient quality. For instance, it remains difficult to ascertain very long term intensity changes [3] and to untangle with some confidence any evolution linked to changes in geomagnetic reversal frequency (e.g., see [4]). The sawtooth pattern apparently seen in relative paleointensity from sediments [5] has also not yet been

* Corresponding author. Tel.: +33 1 4511 4184; fax: +33 1 4511 4190.
E-mail address: legoff@ipgp.jussieu.fr (M. Le Goff).

0012-821X/$ - see front matter © 2004 Elsevier B.V. All rights reserved.
doi:10.1016/j.epsl.2004.10.025

satisfactorily tested from absolute intensity determinations. These uncertainties clearly leave open the possibility that some important properties of the geomagnetic field could actually be unknown.

The scarcity of the absolute intensity data obtained either from volcanic rocks or baked archeological materials mainly results from the fact that most available investigation procedures are laborious and often unproductive due to poor data quality. The principal method, relying on the additive property of partial TRM (pTRM), was proposed by Thellier and Thellier [2]. It consists of progressively replacing the original TRM (i.e., the natural remanent magnetization NRM) by a new one acquired under known laboratory field conditions. Although rather old, this method and its principal variant [6] are generally considered the most reliable paleo-intensity techniques, as long as tests for judging magnetic mineralogy stability with the heating of the samples are conducted. In these experiments, the samples are repeatedly heated to increasing temperatures, with typically ~20 to 30 heating–cooling cycles lasting at least 1 h each. Such a time-consuming procedure requires a large amount of magnetization measurements but often has a poor success rate because of mineral alteration during heating. To diminish the time of heating and hopefully the possibility for alteration, Shaw [7] proposed a mixed thermal and alternating field (AF) method involving only one heating–cooling cycle at high temperature (~600 °C). In this method, the NRM is demagnetized using alternating fields replaced in one thermal step by a new laboratory "full" TRM which is then also AF demagnetized. This procedure is faster than the previous one, but it is not clear whether the success rate is increased (e.g., see [8]). In most cases, one heating at high temperature is sufficient to significantly alter the magnetic mineralogy of the samples. To better circumvent the problem of alteration, Walton et al. [9,10] proposed a radically different method based on microwave demagnetization. They indeed showed that microwaves emitted at frequencies ≥8 GHz (up to 14 GHz presently) are efficient to quickly and completely demagnetize (and remagnetize) samples without significantly heating the samples (<~150 °C). Several recent studies presented satisfactory comparisons between intensity results obtained rapidly using the microwave technique and much slower using the Thellier and Thellier method (e.g., see [11]). This makes the microwave technique, which is still under technological and methodological development, very promising but rather expensive.

However, we would like to point out the poor understanding of the theory behind microwave technique; a theoretical relationship with Néel's [12] theory of thermal activitation of magnetic moments is not established yet, and thus, the analogy between microwave and thermal remanence magnetization remains based on experimental measurements. For this reason, we have developed another relatively fast procedure, which retains the principal characteristics of the Thellier and Thellier method. We have constructed a new three-axis vibrating sample magnetometer (that we call Triaxe) comprising a small oven placed in the center of a group of 10 pickup coils, all of these being inserted inside three perpendicular Helmholtz coils. This equipment allows continuous high-temperature (up to ~650 °C) magnetization measurements of individual cylindrical ~0.75 cm^3 samples and the acquisition of TRM in any direction and field intensity up to 200 μT. In this first paper, we present a brief description of the instrument, the methodology used to obtain paleo- and archeointensity data and several examples of reliable results obtained in less than 2.5 h.

2. Description of the new instrument

The magnetometer comprises three orthogonal sets of pickup coils necessary for measuring the magnetization of a sample, which vibrates horizontally along a single direction (Fig. 1). Two coaxial coils in opposition are sufficient for detecting the magnetic component along the vibration axis, while two coplanar pairs of coils in opposition are necessary for each perpendicular magnetic component. Both the distance between the coils or the pairs of coils and the size of these coils were carefully designed to insure the most homogeneous and linear electromagnetic effect through the entire displacement volume of the sample. This sensor system is devised for measuring the magnetization of a cylindrical 1-cm-long/1-cm-diameter sample vibrating with a frequency of 11.18 Hz and with a net displacement amplitude of 1 cm. Its sensitivity is better than 10^{-8} Am^2 (~10^{-2} A/m) in all

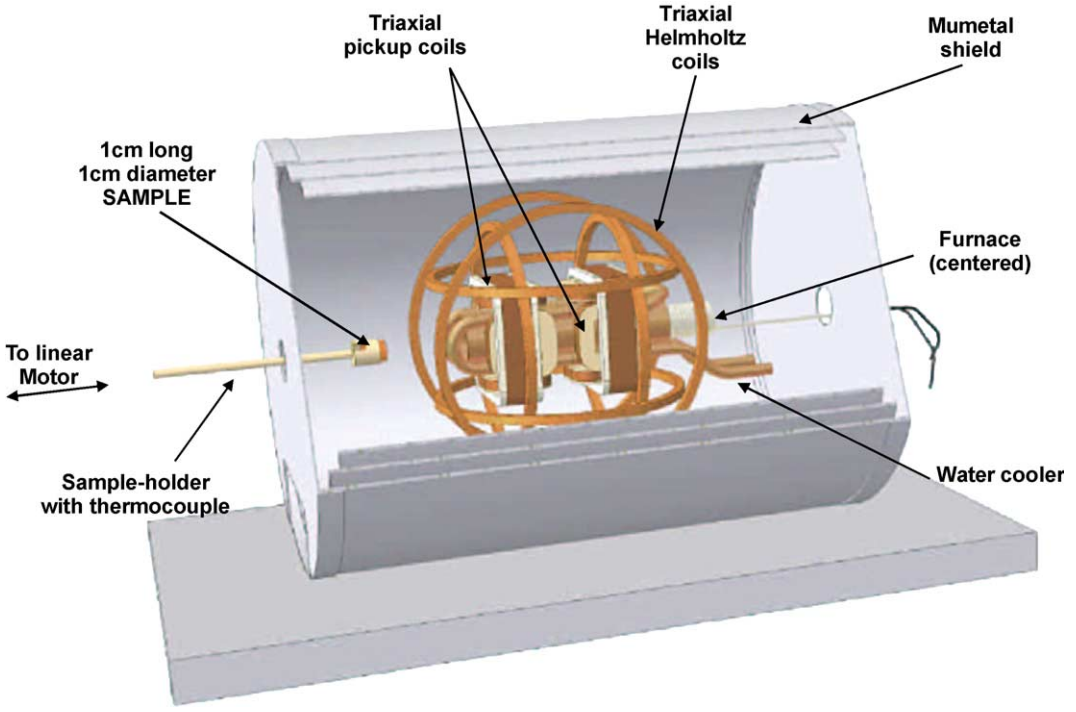

Fig. 1. Schematic of the new three-axis vibrating sample magnetometer. The instrument includes a small oven and its radiator inserted within three orthogonal sets of pickup coils; the whole assemblage is placed inside three Helmholtz coils and a three-layer μmetal shield. This instrument allows continuous high temperature measurements of remanent or induced magnetization for a cylindrical (0.75 cm^3) sample.

three directions, thus allowing magnetization measurements of most volcanic rocks and baked archeological materials. A small oven and its water-cooling system are placed in the center of the pickup coil assembly, that is made easier by the square shape of the 10 coils (Fig. 1). The heating, up to ~650 °C, is produced by a 2.5-kHz alternating current in a bifilar resistor avoiding electromagnetic interference in the pickup coils. The heating and the cooling rates can be adjusted up to a maximum of 60 °C/min. The sensor and heating–cooling systems are centered inside three perpendicular Helmholtz coils coaxial with the magnetometer axes. This permits the generation of a magnetic field up to 200 μT in any direction, in particular, towards the NRM direction of the studied samples. Finally, the complete system except the linear step-by-step motor producing the horizontal sinusoidal displacement of the sample is inserted in a three-layer μmetal cylindrical shield.

We point out that one of the technical difficulties was to ensure the isotropy of both magnetization measurements and field intensity generation together with the best possible alignment between the sensor and Helmholtz coil axes. To test this, we carried out magnetic measurements on a pure paramagnetic sample made of 1 g of Holmium oxide in a field of 150 μT (yielding a magnetization of about ~40.10^{-8} Am^2). These measurements have shown an angular alignment better than 1.5° in all three directions.

3. Methodology used for paleo- and archeo-intensity measurements

There are only a few studies presenting examples of natural TRM measurements at high temperatures in the literature (e.g., see [1,13–17]). We can, however, find a detailed description of intensity determinations from such measurements in Boyd [1] and Tanaka et al. [17]. In the present paper, we will use the high-temperature version of the Thellier and Thellier [2]

method modified by Coe [6], as described in Boyd [1] and Tanaka et al. [17]. Its main difference with the classical method, which involves stepwise magnetization measurements at room temperature, is that it requires, for each studied sample, an investigation of the temperature dependence of the spontaneous magnetization (Js). This is necessary to separate the fraction of magnetization unblocked (or blocked) between two temperatures from the thermal decay of the magnetization fraction remaining blocked.

Between two temperatures T_1 and T_2 (with $T_2>T_1$; Fig. 2), the magnetization is recorded every ~7 s according to the following procedures:

Step 1: The sample is heated in zero field between T_1 and T_2; the magnetization M1(T) is measured (curve 1).

Step 2: The sample is cooled in zero field between T_2 and T_1, providing the magnetization data M2(T) (curve 2).

Step 3: The sample is again heated in zero field to T_2, providing M3(T) (curve 3).

Step 4: At T_2, a field of known intensity and direction (H_{lab}) is applied and maintained while the sample cools to T_1, providing M4 (T) (curve 4).

Step 5: At T_1, the field is turned off, and the sample is heated to T_2, providing M5(T) (curve 5).

Our equipment is able to automatically carry out this whole sequence of measurements. The sample does not need to be manually handled, which increases the directional measurement precision. For intensity computation, we consider only the magnetization data of curves 1, 3 and 5 acquired under the same thermal conditions (i.e., heating curves with the same heating rate) to eliminate the effect of any temperature lag produced by the relatively fast temperature variations.

The behaviour shown by curve 1 reflects both the demagnetization of the NRM between T_1 and T_2 and the thermal evolution of Js of the remaining (blocked) NRM fraction. Of course, as the direction of magnetization is continuously monitored, any

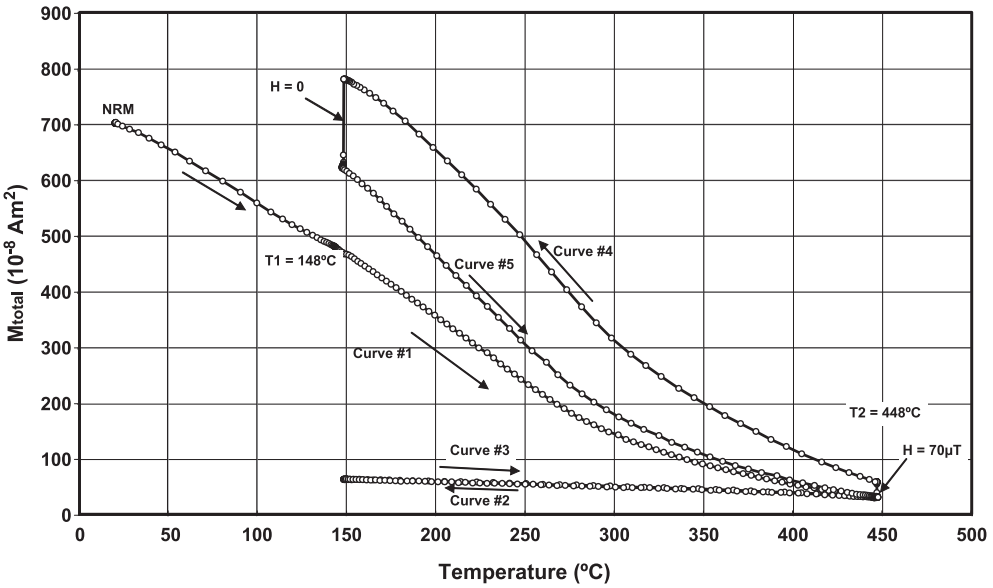

Fig. 2. Example of magnetization data acquired during a complete cycle of measurements for paleo- or archeo-intensity determination. Curve 1 shows the thermal demagnetization between ~150 and ~450 °C of the natural remanent magnetization (NRM) together with the thermal variation of the remaining (blocked) NRM. Curves 2 and 3 show the temperature dependence of the NRM fraction with unblocking temperatures >450 °C. Curves 4 shows the acquisition of a new TRM in a known laboratory field (here 70 μT). Curve 5 is a function of both the thermal demagnetization between ~150 and ~450 °C of the new laboratory TRM and the thermal variation of the remaining laboratory TRM and remaining NRM magnetization fractions.

sample which would show directional variations at this step would be rejected. Curve 5 also shows a combination between the demagnetization (again between T_1 and T_2) of the new TRM imparted during step 4 under a known laboratory field (H_{lab}) and the thermal evolution of Js of the remaining blocked magnetic fraction (laboratory TRM+NRM). Curve 3 represents the temperature dependence between T_1 and T_2 of the NRM fraction with unblocking temperatures $>T_2$.

Hence, at any discrete temperature Ti between T_1 and T_2, the NRM and laboratory TRM fractions ($\Delta 1$(Ti), $\Delta 5$(Ti), respectively) whose unblocking temperatures are between Ti and T_2, are obtained from

$$\Delta 1(\mathrm{Ti}) = M1(\mathrm{Ti}) - M3(\mathrm{Ti}) \quad (1)$$

$$\Delta 5(\mathrm{Ti}) = M5(\mathrm{Ti}) - M3(\mathrm{Ti}) \quad (2)$$

and the ancient field intensity can be derived from the formula

$$R(\mathrm{Ti}) = H_{lab}{*}\Delta 1(\mathrm{Ti})/\Delta 5(\mathrm{Ti}) \quad (3)$$

Another possibility neither explored by Boyd [1] nor Tanaka et al. [17] is to estimate the NRM and laboratory TRM fractions unblocked between T_1 and Ti. In contrast with the previous computations for which we compare two pTRM at the same temperature Ti (see Eqs. (1) and (2)), we now consider the decrease in magnetization between two temperatures T_1 and Ti, thus including both the demagnetization of the pTRM and the thermal dependence of Js. These computations require us to make an approximation because the variation in Js between T_1 and Ti of the magnetic fraction with unblocking temperatures between Ti and T_2 is not known. There are two possibilities. The first is to consider that the behaviour of the curve 3 between T_1 and Ti provides a proxy for the Js variation. We then can write:

$$\Delta 1'\ (\mathrm{Ti}) = M1(\mathrm{T_1}) - (M3(\mathrm{T_1})/M3(\mathrm{Ti})){*}M1(\mathrm{Ti}) \quad (4)$$

$$\Delta 5'\ (\mathrm{Ti}) = M5(\mathrm{T_1}) - (M3(\mathrm{T_1})/M3(\mathrm{Ti})){*}M5(\mathrm{Ti}) \quad (5)$$

As the remaining fraction above T_2 is small, the second possibility is to simply neglect the variation in Js because $M3(T)$ does not provide the necessary constraints. In this case:

$$\Delta 1'\ (\mathrm{Ti}) = (M1(T_1) - M1(\mathrm{Ti})) - (M3(T_1) - M3(\mathrm{Ti})) \quad (6)$$

$$\Delta 5'\ (\mathrm{Ti}) = (M5(T_1) - M5(\mathrm{Ti})) - (M3(T_1) - M3(\mathrm{Ti})) \quad (7)$$

In both cases, the ancient field intensity can be obtained from:

$$R'\ (\mathrm{Ti}) = H_{lab}{*}\Delta'\ 1(\mathrm{Ti})/\Delta 5'\ (\mathrm{Ti}) \quad (8)$$

It is worth noting that experiments carried out on several archeological samples show that the differences in R' (Ti) induced by the two possibilities of computations are very small (and especially negligible when the variation of $M3(T)$ is linear). In the present study, we prefer to not consider any proxy for the Js variation between T_1 and Ti, and we use Eqs. (6) and (7) to compute the ratio R' (Ti).

Practically, both computations of R(Ti) and R' (Ti) require the interpolation of the three data sets $M1(T)$, $M3(T)$ and $M5(T)$ to obtain data at the same temperature Ti. A temperature interval of 5 °C is chosen, which is very close to the mean interval of actual measurements.

4. Testing the experimental procedure on laboratory TRM

Fig. 3 shows several examples of continuous intensity measurements from a pottery sample (always the same). In all cases, a pseudo ancient magnetization (NRM) was first acquired with a maximum temperature of 500 °C in a field of 50 μT. We will see in the next section that the cooling rate during the acquisition of laboratory TRM is an important parameter in these experiments. In these first examples, we simply use a rapid and constant cooling rate of 25 °C/min for the acquisition of both "NRM" and laboratory TRM. An identical pause time of 5 min is used when the laboratory field is turned on at T_2 (at the beginning of step 4) and when it is turned off at T_1 (beginning of step 5). We report in Fig. 3 the values of R(Ti) and R' (Ti) (curves with solid and open symbols, respectively) obtained with measurements every 5 °C

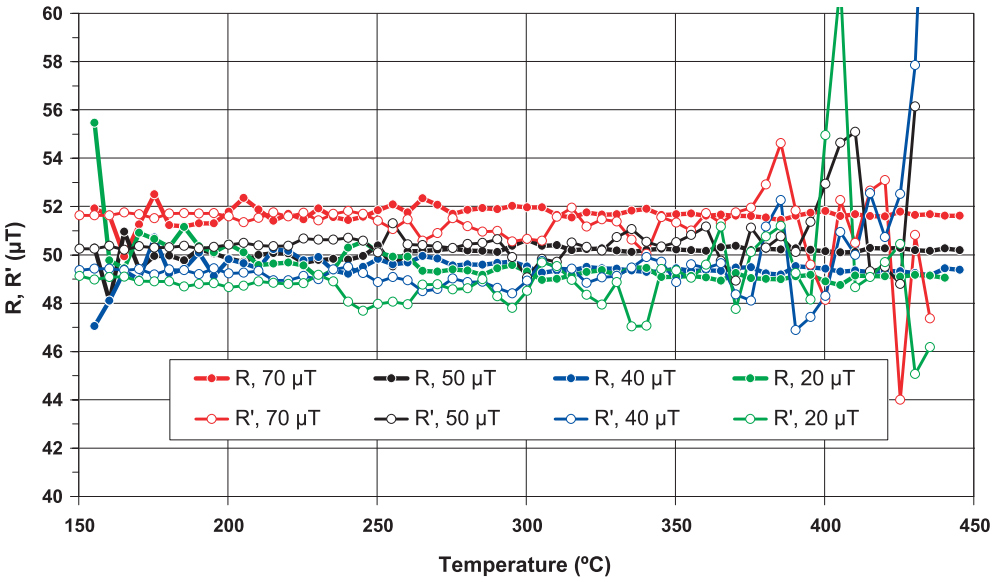

Fig. 3. Examples of continuous intensity measurements from a pottery sample in which a pseudo ancient NRM was first acquired up to 500 °C in a field of 50 μT. The "ancient" field intensity is determined using laboratory fields of 20 μT (green), 40 μT (blue), 50 μT (black) and 70 μT (red). Note that both the NRM and the laboratory TRM are acquired in the same thermal conditions (i.e., same heating and cooling rates). For each applied laboratory field, estimates of the "ancient" field intensity are derived every 5 °C between 150 and 450 °C from two ratios R(Ti) and R' (Ti) (curves with solid and open symbols, respectively). See text for explanations.

between 150 and 450 °C using successively a laboratory field of 20 μT (curves in green), 40 μT (blue), 50 μT (black) and 70 μT (red). In each case, the values are quite constant over a large segment of the 300 °C temperature interval, but the raw R(Ti) data are scattered at the higher temperatures (last ~70 °C), while the R' (Ti) data are scattered but much less at the lower temperatures (first ~30 °C). This scatter reflects the increased importance of noise as the magnetization fractions involved in the ratio computation diminish. The problem is even worse for R(Ti) because of the uncertainties existing in the determination of $M1(T_2)$, $M3(T_2)$ and $M5(T_2)$. These three values, which should remain exactly the same during all the experiment, may however be affected by a very small drift. The resulting effect may not be negligible when the differences $M1(T)-M3(T)$ and $M5(T)-M3(T)$ are small. Even if this effect is rarely important, we recalculate values at T_2 from the smoothing of the final one-third of the three curves, and we simply shift $\Delta 1(Ti)$ and $\Delta 5(Ti)$ by $M1(T_2)-M3(T_2)$ and $M5(T_2)-M3(T_2)$, respectively.

The mean intensity values computed from the previous R(Ti) (between 150 and 380 °C) and R' (Ti) data (between 180 and 450 °C) are very close to the field intensity used to generate the NRM (respectively, 48.7±0.7 and 49.4±0.5 for 20 μT, 49.1±0.4 and 49.4±0.3 for 40 μT, 50.3±0.4 and 50.1±0.2 for 50 μT, 51.4±0.4 and 51.7±0.2 for 70 μT). In all cases, the concordance is within 5%, which validates the experimental method proposed to determine the ancient field intensity. We however remark that the closer the laboratory field intensity to the "ancient" field intensity, the better the agreement between the intensity determination and the "ancient" field intensity. In other words, our experiments indicate that the laboratory field must be adjusted as close as possible to the expected ancient field intensity (see also [18–20]). The origin of this relatively small but clearly identified effect will be the subject of further studies.

5. The cooling rate effect

Genevey and Gallet [21] recently emphasized the importance of experimentally estimating the cooling rate dependence of TRM acquisition for obtaining more reliable archeo-intensity determinations (see

also [22]). This effect is due to the fact that the baked clay samples are cooled much more rapidly during laboratory experiments than during their original firing (the latter cooling could have lasted several days), which generally leads to an overestimation of the ancient field intensity [23–25].

In our experiments using baked clay samples, the cooling rate effect can be illustrated by comparing the values of the ratio R(Ti) (curves with solid symbols in Fig. 4) obtained using successively a rapid (25 °C/min, black curve), a moderate (6 °C/min, blue curve) and a slow (2 °C/min, green curve) cooling rate during the laboratory TRM acquisition (step 4) in all cases from the same initial conditions (a TRM acquired in the same sample up to 500 °C in a field of 50 μT and after a cooling time of 16 h). The three R(Ti) data sets are determined between 150 and 450 °C. When the sample is rapidly cooled, the values significantly and smoothly increase with increasing temperatures starting at 150 °C from a slightly overestimated field intensity value in comparison with the expected intensity and reaching strongly biased values at high temperatures. This increasing trend is progressively lowered when slower cooling rates are considered, but it still exists for the cooling rate of 2 °C/min (to be compared with the cooling rate of 0.5 °C/min for the acquisition of the pseudo ancient NRM). We also observe that the initial intensity value obtained at 150 °C becomes closer to the expected field intensity as the cooling rate is decreased. The cooling rate effect can also be illustrated by showing the $R(T)$ data when the cooling rate used for TRM acquisition is slower than the one applied for NRM acquisition (6 and 60 °C/min, respectively). In clear contrast with the previous cases, the values now show a significant decreasing trend (red curve).

An option would be naturally to consider a very slow cooling rate for the laboratory TRM acquisition, but this would imply an unreasonably long duration for intensity determinations. It is worth pointing out that the trends in R(Ti) reflect the fact that the bias produced by the small quantity of TRM not gained between T_2 and T_1 because of a too rapid cooling rate becomes stronger as the magnetization fractions with unblocking temperatures between Ti and T_2 progressively diminish with increasing temperatures Ti. This difficulty can be bypassed by considering the ratio R' (Ti) which involves the magnetization fractions

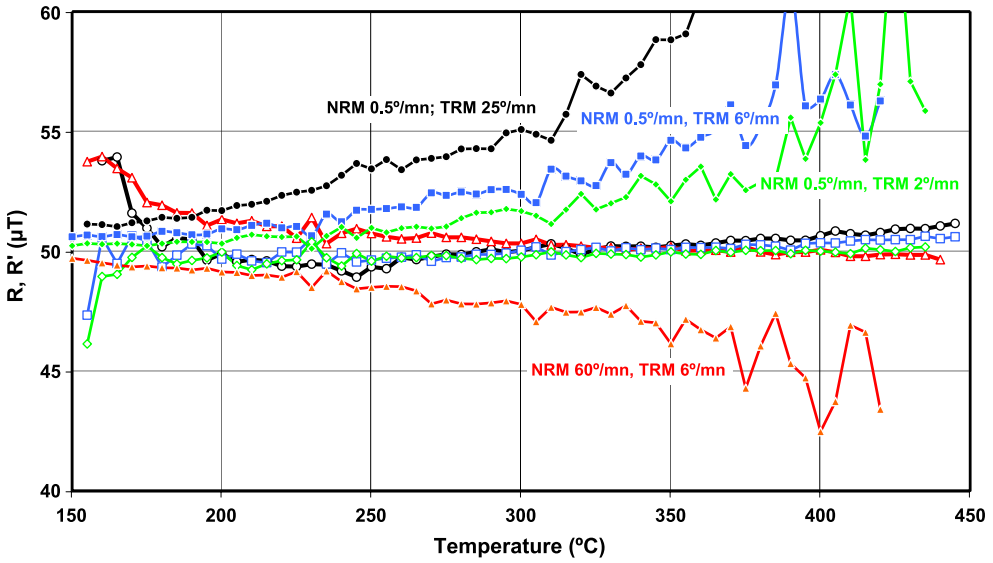

Fig. 4. Effect of the cooling rate dependence of TRM acquisition in our experiments. We show the estimates of the pseudo ancient field intensity given by R(Ti) and R' (Ti) (curves with solid and open symbols, respectively) obtained every 5 °C between 150 and 450 °C using a rapid (25 °C/min; in black), a moderate (6 °C/min; in blue) and a slow (2 °C/min; in green) cooling rate for the laboratory TRM acquisition (in a field of 50 μT). In these three cases, the same initial NRM imparted in the same sample is analyzed (acquired up to 500 °C in a field of 50 μT and after a long cooling time of 16 h). A fourth case (curves in red) shows the behaviour when the laboratory TRM is acquired much slowly than the NRM (6 and 60 °C/min, respectively). See text for further description and explanation.

unblocked between T_1 and Ti (thus increasing with temperature). The values obtained for this ratio are indeed in much better agreement with the expected field intensity (Fig. 4). For each used cooling rate, the most biased intensity value is observed at T_2 (being necessarily equal to the one obtained for R(Ti) at Ti=T_1). However, whatever the cooling rate, the recovered intensity values are almost identical to the expected intensity over a large part of the temperature interval. Our experiments thus indicate that R' (Ti) provides a reliable estimate of the ancient field intensity fairly independent of the cooling rate effect, even when a cooling rate as fast as 25 °C/min is used for laboratory TRM acquisition. The use of a slower cooling rate appears unnecessary. This makes possible a complete field intensity determination in less than 2.5 h for one sample.

6. Anisotropy of TRM

The anisotropy of TRM is known to be important in most baked archeological materials (e.g., see [21,22,26–28]). It has been demonstrated by the fact that the direction of the TRM acquired by a baked clay artifact, such as a brick or a pottery, is often different from the direction of the applied field. This deflection is generally consistent with the existence of an easy plane of magnetization induced by the manufacturing process (i.e., identical to the stretching plane). In the usual procedure with magnetization measurements at room temperature, the TRM anisotropy effect is estimated for each sample by measuring partial TRM acquired successively in six directions, which allows the determination of the TRM anisotropy tensor. A TRM anisotropy factor is then computed [29] and used to correct the raw intensity value. Another method consists in producing a TRM closely in the direction (within 10°) of the original magnetization (NRM), which avoids the need to quantify and correct the magnetization data for TRM anisotropy (e.g., see [26,27]). In most cases, except when the TRM anisotropy is too strong, this is possible by simply applying the laboratory field in the direction of the NRM.

In our experiments, we use an automatic procedure that always yields laboratory TRM with a direction nearly identical to that of the NRM. Fig. 5a,b shows the principle of this procedure.

For a unit field H_{ancient} applied in the direction Ω from the maximum anisotropy axis $k_{\max}$ of eigenvalue $k>1$ (the eigenvalue $k_{\min}$ being the unit), the direction β of NRM can be computed from

$$\beta = \operatorname{atan}(\sin\Omega/k\cos\Omega) \tag{9}$$

and the unit NRM magnetization from

$$M_{\text{NRM}} = (\sin^2\Omega + k^2\cos^2\Omega)^{1/2} \tag{10}$$

If the laboratory field is applied in the NRM direction β, we can calculate β', the direction of the laboratory TRM, from Eq. (9) with $\Omega=\beta$ and then the angle $\gamma=\beta-\beta'$ (Fig. 5a,b). The ratio $M_{\text{TRM}}/M_{\text{NRM}}$ is thus

$$M_{\text{TRM}}/M_{\text{NRM}} = (\sin^2\beta + k^2\cos^2\beta)^{1/2}/M_{\text{NRM}} \tag{11}$$

This ratio is always larger than 1 (see Fig. 5b).

The curves computed in Fig. 5b for a large anisotropy factor k=1.5 indicate that, depending on the initial direction Ω, γ can be larger than 10°, which induces an overestimate of the ratio $M_{\text{TRM}}/M_{\text{NRM}}$ by ~7%. In addition, our computations demonstrate that, independent from the anisotropy factor k, if the angle $\gamma<4°$ then $M_{\text{TRM}}/M_{\text{NRM}}$ does not differ by more than 1%. For larger γ, the correction of the applied field direction by $-\gamma$ leads to the acquisition of a laboratory TRM within 3° of the NRM direction, and the ratio $M_{\text{TRM}}/M_{\text{NRM}}$ is not biased by more than 1.5%.

Therefore, at the beginning of step 4, (1) the laboratory field is first applied parallel to the NRM, (2) the direction of the laboratory TRM is determined over a limited temperature interval (~one-tenth of the T_2–T_1 interval) and compared to the NRM direction to obtain γ, (3) if $\gamma<4°$, the TRM acquisition is done up to T_1 because the TRM anisotropy effect can reasonably be neglected, (4) if $\gamma>4°$, a new direction is computed for the applied field by rotating its previous direction by $-\gamma$, the sample is again heated to T_2. The normal procedure resumes with a laboratory TRM acquisition in a field pointing towards the recalculated direction. It is worth noting that the time

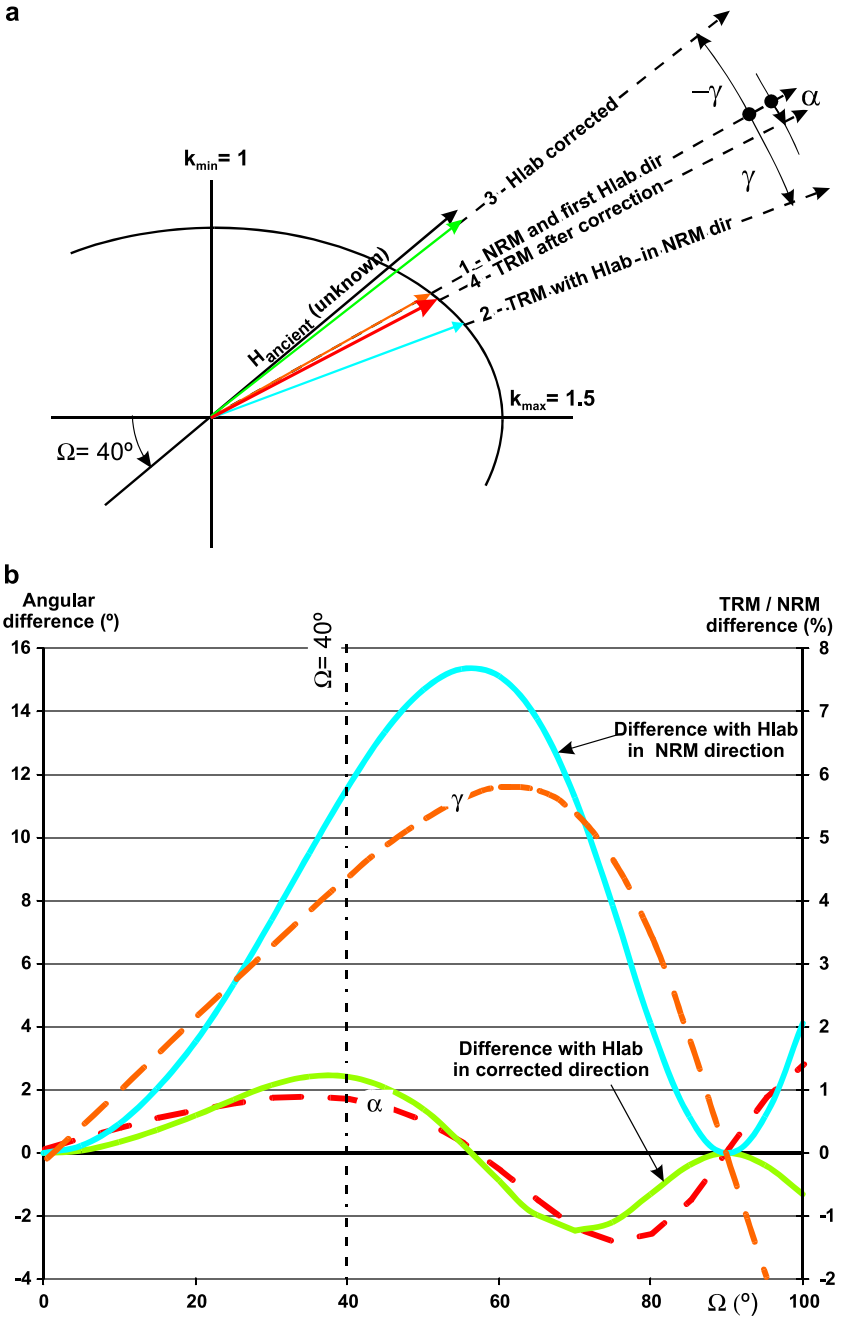

Fig. 5. Description of the procedure used to correct intensity determinations for the anisotropy of TRM. The considered example has a TRM anisotropy factor of 1.5. Panel (a) illustrates the anisotropy of TRM which causes a discrepancy between the direction of the laboratory TRM and the NRM. γ is the angle between the TRM and the NRM. If γ is significant (>4°), we correct the direction of the applied field by $-\gamma$. Panel (b) presents the computations of the angular differences between the NRM and the laboratory TRM (curve "γ" and "α," respectively) and of the variations in the ratio $M_{\mathrm{TRM}}/M_{\mathrm{NRM}}$ (blue and green curve, respectively) before and after correcting the direction of the applied field by $-\gamma$.

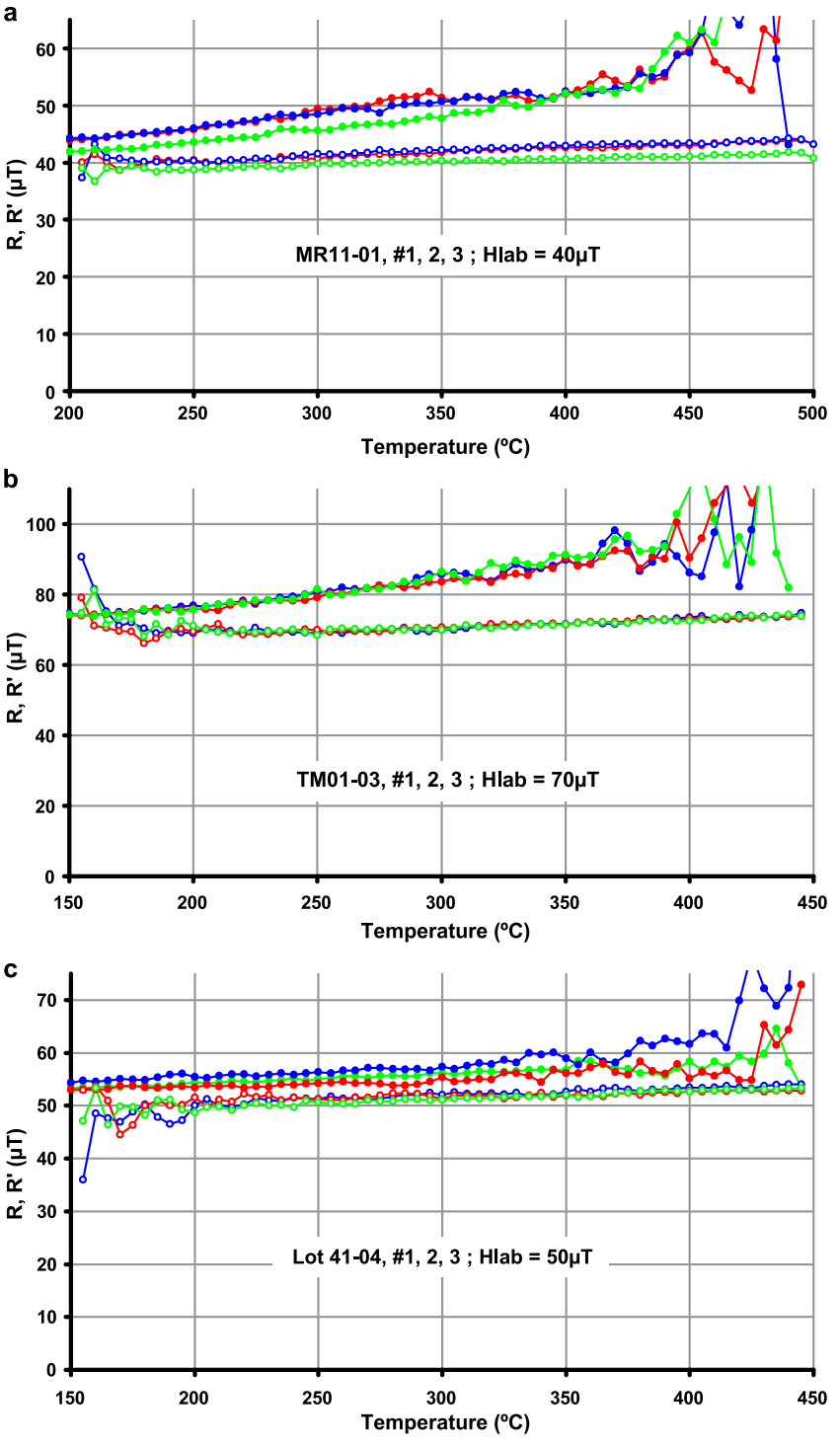
a
R, R' (μT)
MR11-01, #1, 2, 3 ; Hlab = 40μT
Temperature (ºC)
b
R, R' (μT)
TM01-03, #1, 2, 3 ; Hlab = 70μT
Temperature (ºC)
c
R, R' (μT)
Lot 41-04, #1, 2, 3 ; Hlab = 50μT
Temperature (ºC)

Table 1
Archeo-intensity values determined from our new experimental procedure and comparison with the data previously obtained by Genevey et al. [28] from the same three archeological fragments and from their corresponding sites. These latter results ($H_{fragment}$ and H_{site}, respectively) are corrected both for TRM anisotropy and cooling rate dependence of TRM acquisition. Each new archeo-intensity value ($H_{specimen}$) is given by the mean of the R'_{Ti} data obtained every 5 °C over a ~300 °C temperature interval

Fragment	Sample	T_{min}–T_{max} [°C]	H_{lab} [μT]	H_{sample} [μT]	H_{mean} [μT]	$H_{fragment}$ [μT] (Genevey et al. [28])	H_{site} [μT]
MR11-01	1	200–500	40	40.8±0.5			
	2	200–500	40	40.2±0.9	40.9±0.8	40.9±0.9	43.4±2.2
	3	200–500	40	41.8±1.3			
TM01-03	1	150–450	70	71.1±1.7			
	2	150–450	70	71.3±1.5	71.2±0.1	70.3±0.3	71.6±4.3
	3	150–450	70	71.2±1.6			
Lot41-04	1	150–450	50	51.1±1.1			
	2	150–450	50	51.8±1.8	51.4±0.3	54.2±0.7	50.4±3.1
	3	150–450	50	51.4±1.4			

necessary for correcting the TRM anisotropy effect is less than 10 min.

7. Discussion and conclusion

To further test the new method, we have analysed three archeological fragments from Mesopotamia, previously studied by Genevey et al. [28] using the classical Thellier and Thellier [2] method modified by Coe [6]. Each fragment gave reliable and consistent archeo-intensity results both at the fragment level (two specimens were analysed per fragment) and at the site level (several fragments of the same age and found in the same archeological context were analysed). Fig. 6 shows the results obtained from three specimens taken per fragment (Fig. 6a, MR11-01; Fig. 6b, TM01-03; Fig. 6c, Lot 41-04). For these experiments, the laboratory field was closely adjusted to the archeo-intensity results obtained by Genevey et al. [28], and the cooling rate for laboratory TRM acquisition was always 25 °C/min. In each case, we report the values of R(Ti) and R' (Ti) determined every 5 °C over a temperature interval of 300 °C. The curves obtained from each fragment are very consistent and show behaviors very similar to those described in the previous section. Whereas the R(Ti) values significantly increase with increasing temperatures (curves with solid symbols), the R' (Ti) values (curves with open symbols) are more stable with only a slight increasing trend. For each sample, we have therefore simply computed the mean of the R' (Ti) values over the entire temperature interval with the exception of the "noisy" first 20 °C. Then for each fragment, we have averaged the three mean values to estimate the ancient field intensity. The individual results (i.e., at the sample level) obtained from each fragment are all within 3% of the mean (H_{mean}; Table 1). The comparison of the means with the expected intensity values (after corrections for anisotropy and cooling rate effects) shows differences which in two cases (MR11-01, Fig. 6a, and TM01-03, Fig. 6b) do not exceed 5% (~0% and +1%, respectively). The difference is −5.2% for fragment Lot41-04 (Fig. 6c), but in all cases, the new intensity estimates are within the error bars previously obtained at the site level (Table 1). We therefore consider very satisfactory the comparison between the two data sets, the small differences being related to usual experimental uncertainties.

Finally, we show a pottery sample which does not permit the determination of an intensity value (Fig. 7). Both R(Ti) and R' (Ti) exhibit strong variations, which are quite different from those previously described and cannot be explained by the cooling rate effect (neither

Fig. 6. Examples of ancient field intensity determination. The results are obtained from series of three specimens taken from three different archeological fragments ((a) MR11-01; (b) TM01-03; (c) Lot41-04). For these analyses, the laboratory field is adjusted to the archeo-intensity results obtained by Genevey et al. [28], and in all cases, the cooling rate for laboratory TRM acquisition is 25 °C/min. For each studied sample, we report the values of $R(T)$ and R' (T) (curves with solid and open symbols, respectively) determined every 5 °C over a temperature interval of 300 °C.

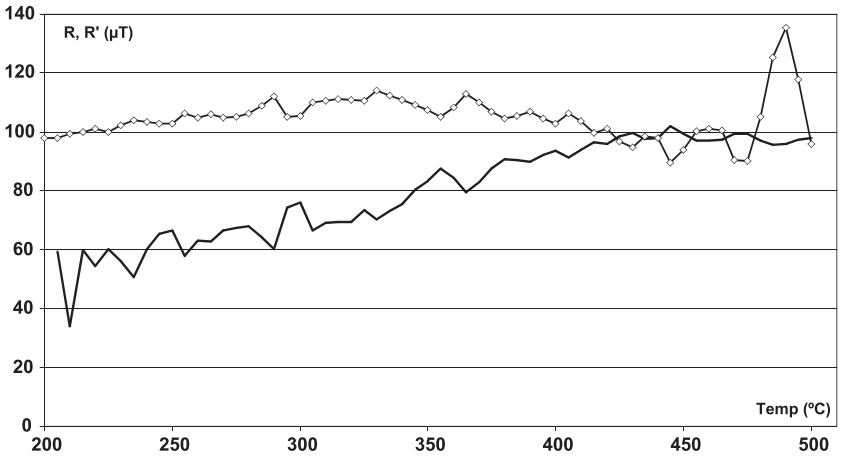

Fig. 7. Example of sample which fails in the determination of an ancient field intensity most probably because of chemical alteration during heating. The cooling rate for laboratory TRM acquisition is 25 °C/min. Same conventions as in Figs. 4 and 6.

of course by directional variations during the NRM demagnetization). In particular, the R' (Ti) data vary significantly over the entire temperature interval leading to the rejection of the sample. Such behaviour is most probably caused by chemical alteration during the treatment. Problems related to chemical alteration, which normally prevent the determination of reliable intensity data, will be addressed in a subsequent study.

These first results illustrate the promising potential of the new magnetometer for paleo- and archeointensity studies studies. The automatic experimental procedure described in Sections 3 and 6 provides reliable intensity data, both corrected for cooling rate dependence of TRM acquisition and TRM anisotropy in less than 2.5 h each. All experiments presented in this study were carried out using baked clay samples for which, in most cases, the cooling rate effect favours the ratio R' (Ti). Moreover, in these samples, the magnetization is generally unblocked at relatively low temperatures (~<500 °C). Further studies are now envisioned to employ the new method on volcanic rocks with higher unblocking temperature spectra and to investigate rock magnetic properties at high temperatures.

Acknowledgements

This work is dedicated to the memory of Professor Emile Thellier who introduced Maxime Le Goff to the pleasures of instrumentation and experimentation in rock magnetism.We are grateful to Philippe Vidal who had enough confidence in us to give us financial support. We thank Thierry Poidras (CNRS, University Montpellier II) who participated in designing the system producing the displacement of the sample. We thank Brian Carter-Stiglitz, Özden Özdemir, David Dunlop, Vincent Courtillot, Agnès Genevey and Stuart Gilder for helpful discussions and comments on the manuscript. The manuscript also benefited from reviews of B. Weiss and an anonymous referee. The construction of the new magnetometer was supported by CNRS (INSU, IT-Dyeti program).This is IPGP contribution no. 2018 and INSU no. 372.

References

[1] M. Boyd, A new method for measuring paleomagnetic intensities, Nature 319 (1986) 208–209.
[2] E. Thellier, O. Thellier, Sur l'intensité du champ magnétique terrestre dans le passé historique et géologique, Ann. Geophys. 15 (1959) 285–376.
[3] M. Macouin, J.P. Valet, J. Besse, Long-term evolution of the geomagnetic dipole moment, Phys. Earth Planet. Inter. 147 (2004) 239–246.
[4] R. Heller, R. Merrill, P. McFadden, The variation of intensity of earth's magnetic field with time, Phys. Earth Planet. Inter. 131 (2002) 237–250.
[5] J.–P. Valet, L. Meynadier, Geomagnetic field intensity and reversals during the past four million years, Nature 366 (1993) 234–238.

[6] R. Coe, Paleo-intensities of the earth's magnetic field determined from Tertiary and Quaternary rocks, J. Geophys. Res. 72 (1967) 3247–3262.
[7] J. Shaw, A new method of determining the magnitude of the paleomagnetic field, Geophys. J. R. Astron. Soc. 39 (1974) 133–141.
[8] J. Morales, A. Gogichaishvili, J. Urrutia, An experimental evaluation of Shaw's paleointensity method and its modifications using late Quaternary basalts, Geophys. Res. Abstr. 5 (2003) 01479.
[9] D. Walton, J. Shaw, J. Share, J. Hakes, Microwave demagnetization, J. Appl. Phys. 71 (1992) 1549–1551.
[10] D. Walton, J. Share, T. Rolph, J. Shaw, Microwave magnetisation, Geophys. Res. Lett. 20 (1993) 109–111.
[11] J. Shaw, S. Yang, T. Rolph, F. Sun, A comparison of archaeointensity results from Chinese ceramics using microwave and conventional Thellier's and Shaw's methods, Geophys. J. Int. 136 (1999) 714–718.
[12] L. Néel, Some theoretical aspects of rock magnetism, Adv. Phys. 4 (1955) 191–243.
[13] K. Burakov, I. Nachasova, A method and results of studying the geomagnetic field of Khiva from the middle of the sixteenth century, Izv. Earth Phys. 14 (1978) 833–838.
[14] D. Walton, Re-evaluation of Greek archaeomagnitudes, Nature 310 (1984) 740–743.
[15] P. Schmidt, D. Clark, Step-wise and continuous thermal demagnetization and theories of thermoremanence, Geophys. J. R. Astron. Soc. 83 (1985) 731–751.
[16] N. Sigiura, Measurements of magnetization at high temperatures and the origin of thermoremanent magnetization: a review, J. Geomagn. Geoelectr. 43 (1989) 3–17.
[17] H. Tanaka, J. Athanassopoulos, J. Dunn, M. Fuller, Paleointensity determinations with measurements at high temperature, J. Geomagn. Geoelectr. 47 (1995) 103–113.
[18] S. Levi, The effect of magnetite particle size on paleointensity determination of the geomagnetic field, Phys. Earth Planet. Inter. 13 (1977) 245–259.
[19] D. Walton, Archaeomagnetic intensity measurements using a SQUID magnetometer, Archaeometry 19 (1977) 192–200.
[20] H. Tanaka, M. Kono, Analysis of the Thellier's method of paleointensity determination: 2. Application to high and low magnetic fields, J. Geomagn. Geoelectr. 36 (1984) 285–297.
[21] A. Genevey, Y. Gallet, Intensity of the geomagnetic field in Western Europe over the past 2000 years: new data from French ancient pottery, J. Geophys. Res. 107 (2002) 2285.
[22] A. Chauvin, Y. Garcia, P. Lanos, F. Laubenheimer, Paleointensity of the geomagnetic field recovered on archaeomagnetic sites from France, Phys. Earth Planet. Inter. 120 (2000) 111–136.
[23] J. Fox, M. Aitken, Cooling-rate dependence of thermoremanent magnetization, Nature 283 (1980) 462–463.
[24] M. Dodson, E. McClelland-Brown, Magnetic blocking temperatures of single-domain grains during slow cooling, J. Geophys. Res. 85 (1980) 2625–2637.
[25] S. Halgedahl, R. Day, M. Fuller, The effect of cooling rate on the intensity of weak-field TRM in single-domain magnetite, J. Geophys. Res. 85 (1980) 3690–3698.
[26] J. Rogers, J. Fox, M. Aitken, Magnetic anisotropy in ancient pottery, Nature 277 (1979) 644–646.
[27] M. Aitken, P. Alcock, G. Bussel, C. Shaw, Archaeomagnetic determination of the past geomagnetic intensity using ancient ceramics: allowance for anisotropy, Archaeometry 23 (1981) 53–64.
[28] A. Genevey, Y. Gallet, J. Margueron, Eight thousand years of geomagnetic field intensity variations in the eastern Mediterranean, J. Geophys. Res. 108 (2003) 2228.
[29] R. Veitch, I. Hedley, J. Wagner, An investigation of the intensity of the geomagnetic field during Roman times using magnetically anisotropic bricks and tiles, Arch. Sci. 37 (1984) 359–373.